Tuijin Jishu/Journal of Propulsion Technology
ISSN: 1001-4055
Vol. 47 No. 04 (2026)

Synthesis and Characterization of Copper(II) Complex Derived from Chitosan Functionalized Vanillin Thiosemicarbazone and its Anticancer and Antibacterial Studies

Swapnil R. Mouje[1], Pranita U. Gawande[2], Shoeb R. Khan[1], Mayur V. Khedkar*[1]
[1]PG and Research Department of Chemistry, Hislop College,
RTM Nagpur University, Nagpur, 440001, Maharashtra, India
[2]Department of Chemistry, St. Francis De Sales College,
RTM Nagpur University, Nagpur, 440006, Maharashtra, India

Abstract:- Chitosan is an abundant, biocompatible, and biodegradable biopolymer derived from the deacetylation of chitin. To enhance its functional properties for biomedical and environmental applications, chitosan was modified into a Schiff base by reacting its free amino groups with a vanillin, followed by coordination with transition metal Cu ions to form a chitosan Schiff base-metal complex. In addition, their physicochemical and biological properties can be further improved through chemical functionalization, leading to materials with enhanced performance and wider applicability. In this regard, a chitosan-functionalized vanillin thiosemicarbazone ligand and its copper(II) complex were successfully synthesized and characterized using fourier transform infrared spectroscopy, carbon-13 nuclear magnetic resonance spectroscopy, electron spin resonance spectroscopy, X-ray diffraction, thermogravimetric analysis, elemental analysis, and magnetic susceptibility measurements. The results confirmed the successful functionalization of chitosan and coordination of Cu(II) ions with the synthesized ligand. The biological activities of the synthesized compounds were examined using antibacterial and anticancer assays. Antibacterial activity was evaluated against pathogenic bacterial strains using the Kirby–Bauer well-diffusion method at different concentrations. The Cu(II) complex exhibited better antibacterial performance than the free ligand. Furthermore, MTT assay results against the MCF-7 breast cancer cell line revealed enhanced anticancer activity after complexation with Cu(II) ions. The improved biological performance of the Cu(II) complex highlights its potential as a chitosan-based biomaterial for therapeutic application.

Keywords: Biopolymer, Chitosan, Thiosemicarbazone, Vanillin, Thiosemicarbazone Cu(II) complex, Anticancer activity.

1. Introduction

In recent years, considerable emphasis has been given to the development of greener, cleaner, and more sustainable chemical processes. These efforts aim to reduce the environmental impact of industrial chemistry through the utilization of biologically derived materials and minimization of pollution and contamination. Biopolymers have emerged as promising materials owing to their biodegradability, renewability, and natural abundance. Consequently, they have found extensive applications in diverse fields such as pharmaceuticals [1], drug delivery [2], agriculture, and environmental science [3] owing to their versatility.

Among various biopolymers, chitosan is the second most abundant naturally occurring linear polysaccharide, obtained through the deacetylation of chitin present in the shells of crustaceans such as shrimp [4], prawns, lobsters, and crabs [5], as well as in fungal cell walls [6]. Chitosan has attracted significant attention because of its unique physicochemical properties and biological activities [7]. Structurally, chitosan consists of β-(1→4)-

linked D-glucosamine and N-acetyl-D-glucosamine units. The amino and hydroxyl groups present in the repeating glucosamine units serve as active sites for chemical modification.

Among the reported chemical modifications, imine functionalization of chitosan has gained considerable interest because it leads to the formation of Schiff bases (SBs). Chitosan can be readily functionalized through condensation of its primary amino groups with aromatic aldehydes such as salicylaldehyde [8], dimethylaminobenzaldehyde [9], o-anisaldehyde, and cinnamaldehyde [10], resulting in the formation of chitosan-based Schiff bases (CSBs). Such chemical modifications provide an effective approach for controlling the interaction of chitosan with other components, including metal ions and biologically active organic molecules such as drugs. Furthermore, chemical functionalization improves the bulk properties of chitosan and enhances its application in sustained drug delivery systems, antimicrobial activity, catalysis, adsorption, and metal complexation [11].

The extensive applicability of functionalized chitosan has encouraged researchers to develop various modified chitosan derivatives by incorporating different organic moieties [12,13], among which chitosan thiosemicarbazone derivatives constitute an important class [14]. Thiosemicarbazones are a class of N, S-donor organic compounds known for their remarkable biological activities, particularly their ability to inhibit DNA biosynthesis [15,16]. Owing to these unique characteristics, Adhikari et al. explored a range of functionalized chitosan thiosemicarbazone derivatives. They reported chitosan thiosemicarbazones derived from various organic compounds, including imidazole-2-carboxaldehyde [17], thiophene [18], pyridine [19], 2-acetylphenol, isatin, and 5-chloroisatin [20] and their copper(II) complexes. These synthesized complexes exhibited notable antitumor activity against the Madin–Darby canine kidney cell line. Yadav et al. reported imidazole-2-thiosemicarbazones [21], and salicylaldehyde and 2-acetylphenol-based chitosan thiosemicarbazones and their copper(II) complexes [22]. In addition to copper, nickel-based chitosan derivatives have attracted attention because of their non-toxicity, biocompatibility, and antioxidant properties. Accordingly, Haj et al. investigated the Ni(II) complex of chitosan thiosemicarbazone for anticancer activity [23].

The literature clearly indicates that thiosemicarbazone-functionalized chitosan and its Cu(II) complexes are promising candidates with significant physicochemical and biological properties. In this context, we report a novel chitosan-functionalized vanillin thiosemicarbazone (CTV) and its Cu(II) complex (CTV–Cu), as illustrated in Scheme 1.

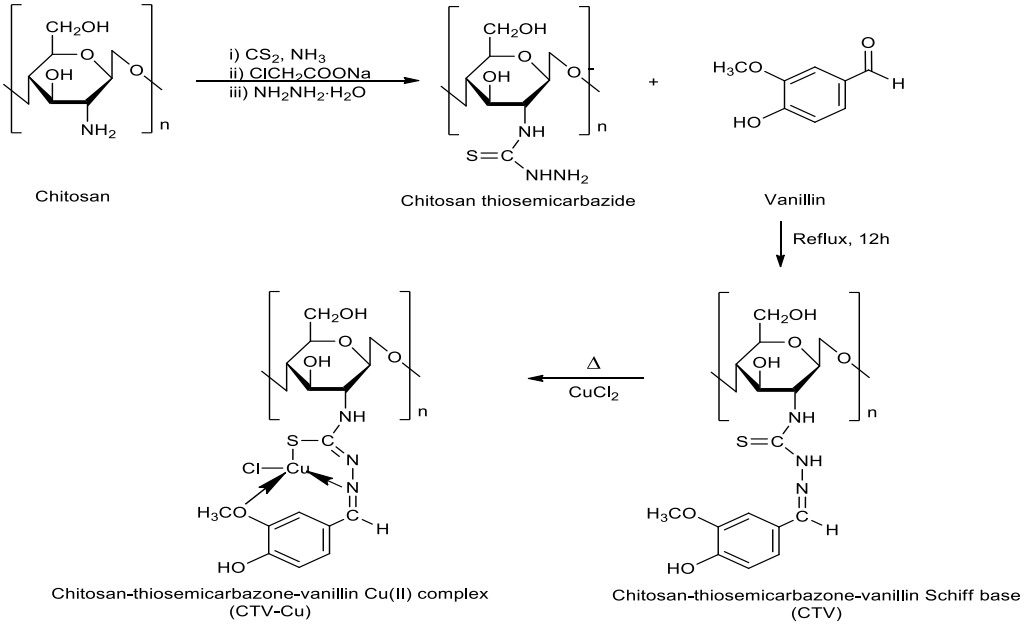
The chitosan-vanillin thiosemicarbazone ligand was synthesized by systematically varying the molar ratio of vanillin to functionalized chitosan to optimize ligand formation and evaluate its chelating performance toward Cu(II) ions. The synthesized CTV ligand and CTV-Cu copper complex was characterized using a combination of analytical and spectroscopic techniques, providing valuable insights into its coordination environment and stability. This study aims to establish a fundamental understanding of the coordination chemistry of chitosan-derived Schiff bases with transition metal ions, thereby facilitating their potential applications in the development of bioactive copper complexes for pharmaceutical, nutraceutical, and materials science applications. These findings are expected to contribute to the advancement and practical utilization of copper-based chitosan complexes as functional materials and potential therapeutic agents.

2. Objectives

The primary objective of this research is to successfully synthesize and characterize a novel chitosan-functionalized vanillin thiosemicarbazone (CTV) ligand and its corresponding copper(II) complex (CTV-Cu) to establish a fundamental understanding of the coordination chemistry between chitosan-derived Schiff bases and transition metal ions. By varying the molar ratio of vanillin to functionalized chitosan, the study aims to optimize ligand formation and evaluate its chelating performance toward Cu(II) ions. Furthermore, the work intends to investigate the physicochemical properties, structural stability, and biological efficacy of the synthesized compounds, specifically assessing their potential antibacterial performance against pathogenic bacterial strains and their anticancer activity against the MCF-7 breast cancer cell line, thereby contributing to the development of advanced bio-based metal complexes for pharmaceutical, nutraceutical, and materials science applications.

3. Methods

The functionalization of chitosan with thiosemicarbazone-vanillin, followed by the formation of its metal complex, was accomplished using a two-step synthetic strategy (Scheme 1). In the first step, thiosemicarbazide was successfully grafted onto the chitosan backbone, followed by condensation with vanillin to yield the CTV ligand. In the second step, the synthesized ligand was reacted with Cu(II) ions to produce the corresponding CTV-Cu complex. This sequential approach ensured efficient ligand formation and effective metal coordination, enabling the development of a structurally robust bio-based metal complex.



Scheme 1. Synthesis of chitosan-functionalized vanillin thiosemicarbazone (CTV) ligand and Cu(II) complex (CTV-Cu).

Step: 1 Preparation of chitosan-vanillin thiosemicarbazone (CTV) ligand

Chitosan (1 g) was stirred with 1.5 mL of ammonia solution in ethanol at room temperature for 1 h. Subsequently, 1 mL of carbon disulfide and 1.42 g of sodium chloroacetate were added to the reaction mixture and stirred for 2 h at room temperature. Next, 1 mL of hydrazine monohydrate was gradually added, and the mixture was stirred at room temperature for 2 h, washed with ethanol, filtered, and dried to obtain a brown chitosan thiosemicarbazide residue. In the next step, the synthesized chitosan thiosemicarbazide was refluxed for 12 h at 65°C with vanillin in the presence of acetic acid as a catalyst. After completion of the reaction, the reaction mixture was filtered, washed with ethanol, and dried. A dark-brown solid was obtained from the CTV ligand.

CTV ligand:- Yield: 68%, color: dark brown; m.p. : 200 °C; elemental analysis (CHNS): C, 18.24; H, 4.20; N, 4.17; S, 1.83%; IR (cm^{-1}, s: strong, m: medium, w: weak): ν(O−H) and ν(N−H) stretch merged with broad absorption at 3265, ν(C=N) 1593s, ν(N−H) bend 1514s, ν(C=S) 1028s, ^{13}C NMR (400 MHz, D_2O, δ): 23.245 (CH_3), 55.984 (C_2), 61.197 (C_6), 74.777–76.623 (C_3, C_5), 98.544 (C_1), 174.637–181.362 (C=S) & (C=O).

Step: 2 Preparation of chitosan-vanillin thiosemicarbazone Cu(II) complex (CTV-Cu)

Chitosan-thiosemicarbazone-vanillin (0.2 g) was dissolved in ethanol (10 mL) and a solution of copper (II) chloride (0.15 g) in ethanol were mixed slowly. The mixture was then stirred and heated for 12 h in a water bath at 60°C; the obtained product was filtered, washed with ethanol, and dried [24].

CTV-Cu Complex: - Yield: 82%; color: light brown; m.p. > 300°C; Elemental Analysis (CHNS): C, 28.67; H, 6.42; N, 6.09; S, 2.00%; IR (cm^{-1}, s: strong, m: medium, w: weak): ν(O−H) and ν(N−H) stretch merged with

broad translocation 3329s, *ν*(C=N) 1626m, *ν*(N−H) bend 1508s, *ν*(C=S) 1066s, effective magnetic moment (μ_{eff}) (B. M): 1.08; ESR (g value): 2.0440 (*ν* = 9.44 GHz, Bo = 0.330 T).

4. Results

FTIR Spectroscopy

The Fourier-transform infrared spectra of the CTV ligand (Figure 1) and CTV-Cu complex (Figure 2) confirmed successful functionalization and metal coordination. The broad translocation of ν(O−H) and ν(N−H) observed in the FT-IR spectra of chitosan vanillin-based thiosemicarbazones (CTV), and its metal complex CTV-Cu at 3265 cm^{-1} and 3329 cm^{-1} respectively. This is attributed to the coaxial stretching vibration of O-H, superimposed on the N-H stretching band, and the intermolecular hydrogen bonding interactions within the polysaccharide matrix. The FT-IR spectrum of CTV-Cu showed a strong band at 1626 cm^{-1}, which is due to the stretching frequency of the azomethine group (-C=N-). The complex spectrum shows a shift in the azomethine stretching frequency. This indicates coordination between the metal center and azomethine nitrogen atom. In addition, the phenolic stretching is shifted to a higher frequency band at 1066 cm^{-1} (Cu) and from 1028 cm^{-1}. The bands arrived at 1070 cm^{-1} in the IR spectra of the Schiff base are due to C-O-C symmetric stretching of methoxy (R-O-CH3). In thiosemicarbazone synthesis, the appearance of ν(N−H) (1504–1556 cm^{-1}) and ν(C=S) (1020–1072 cm^{-1}) bands indicates partial involvement of chitosan NH groups.

The preference for Cu(II) coordination via the methoxy oxygen rather than the phenolic or chitosan backbone hydroxyl groups is driven by both geometric and thermodynamic factors. The spatial orientation of the methoxy group relative to the azomethine nitrogen facilitates the formation of a stable, low-strain membered chelate ring. Furthermore, the hydroxyl groups on the chitosan backbone are structurally restricted within the rigid polymer matrix, making coordination sterically unfavorable compared to the flexible pendant methoxy group. This is supported by the observed shifts in the C-O-C stretching frequencies in the FT-IR spectra upon complexation.

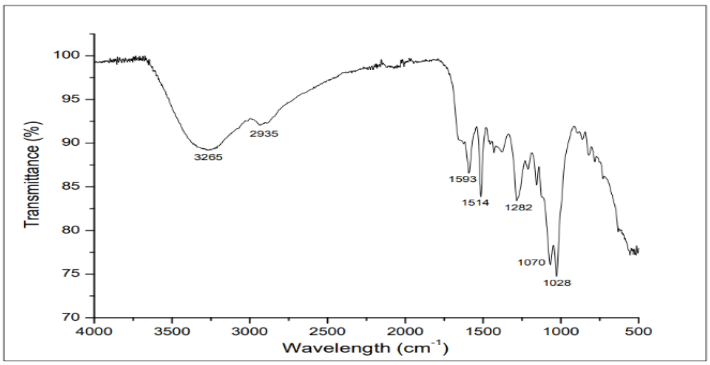


Figure 1. Infrared spectra of CTV ligand.

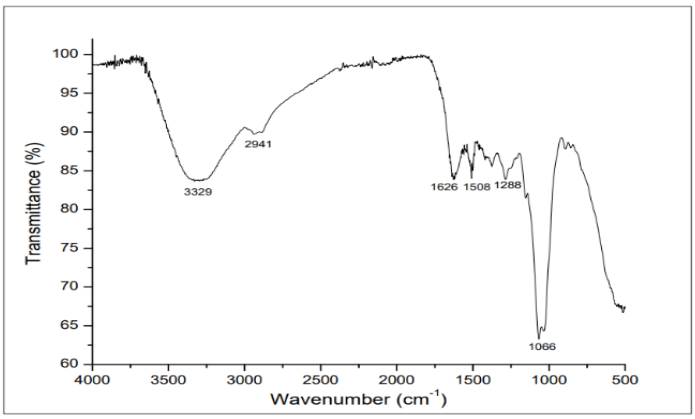


Figure 2. Infrared spectra of CTV-Cu complex.

XRD Analysis

The crystalline nature of the ligand and its metal complexes was evaluated using X-ray diffraction data as shown in Figure 3 and 4, where the 2θ and full width at half maximum (FWHM) values were employed to calculate crystallite sizes according to the Debye–Scherrer equation. The crystallite sizes of the CTV ligand and CTV-Cu complex were calculated using the 2θ values and corresponding FWHM values. The crystal sizes of the CTV ligand and CTV-Cu complex were 46.37 nm and 35.24 nm, respectively. The original crystallinity of chitosan corresponding to the peak was not destroyed, but the crystallinity peaks were weakened and shifted due to the formation of a new crystalline phase, which was attributed to the destruction of hydrogen bonds as a result of the chelation of metal ions with amino or hydroxyl groups in chitosan [25].

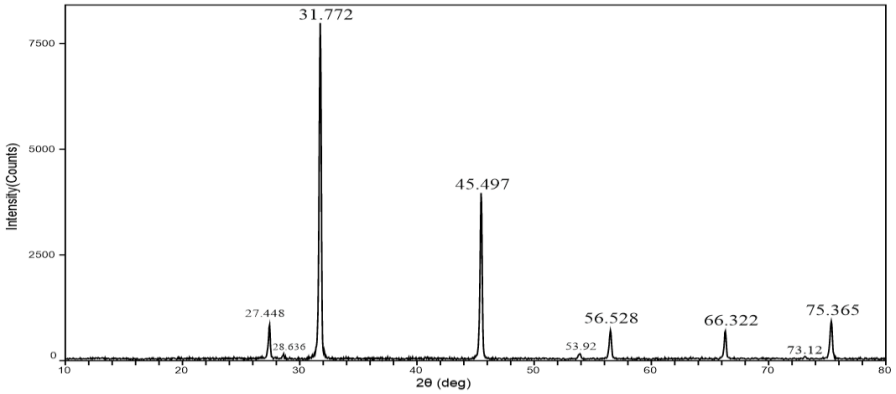


Figure 3. XRD pattern of the CTV ligand.

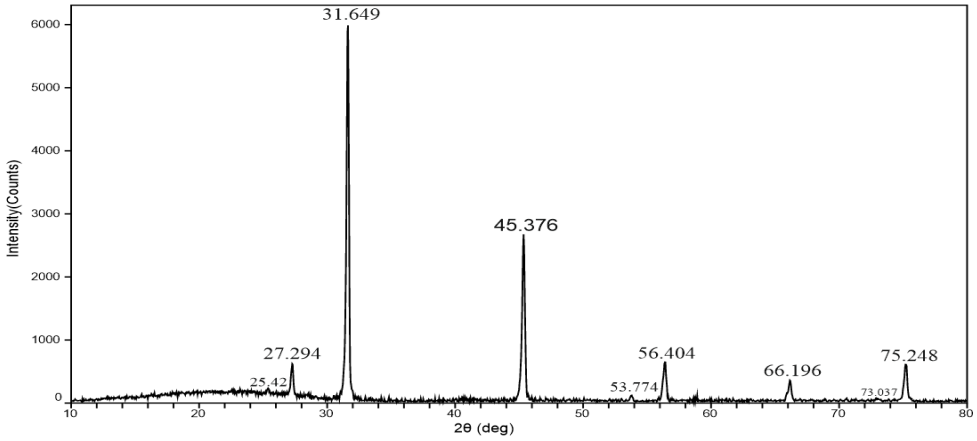


Figure 4. XRD pattern of the CTV-Cu complex.

Thermal Studies

The thermogravimetric/differential thermal analysis (TG/DTA) curves of the CTV and CTV-Cu complex are presented in Figure 5 and 6, respectively, and the thermal data are presented in Table 1. The loss of water at 100-200°C and chain degradation was followed by the disruption of the chitosan backbone in the temperature range of 200-1000°C, which contributed to thermal degradation. There was a weight loss of 6.43% at 185°C due to water loss and a weight loss of 34.57% at 200-900°C due to chain disruption and backbone degradation in CTV.

Considering CTV-Cu complex, there is a weight loss of 7.56% for loss of water at 200°C, a weight loss of 30.10% for disruption of the chain at 200-500°C, and a 5.75% weight loss at 500-700°C for further degradation of the backbone. These thermal events are consistent with studies of chitosan decomposition at 50–100°C and 400–500°C, as well as water loss in chitosan at 80–160°C. Additionally, it has been reported that commercial chitosan

loses weight in two stages: at 120°C, it loses 9% of its weight due to water loss, and at 500°C, it loses 43% of its weight owing to chitosan chain destruction. In accordance with this, the purchased chitosan showed a 13.16% weight loss attributed to the loss of water at 150°C and a 51.70% weight loss due to chain degradation at 500°C. The thermal behavior of thiosemicarbazones according to the higher thermal stability and their DTA peaks showed an agreement with the TG weight loss in two steps of 150−400 and 400−900°C, and an endothermic peak was attributed to the loss of water from 25−150°C.

The initial weight loss of 7.56% observed below 200°C in the CTV-Cu complex is entirely attributed to the evaporation of physically adsorbed and lattice-entrapped water molecules, confirming that the metal complex does not undergo structural decomposition at room temperature. The actual thermal degradation of the coordinated polymeric backbone commences only above 200°C, indicating excellent thermal stability. Furthermore, the synthesized CTV-Cu complex exhibits robust stability under open atmospheric conditions at room temperature; however, dry storage in a desiccator is preferred to mitigate the hygroscopic moisture absorption inherent to the chitosan framework. Regarding its processability, the complex is completely insoluble in water and common organic volatile solvents due to the cross-linking effect induced by Cu(II) coordination, while displaying selective solubility in highly polar coordination solvents such as DMSO.

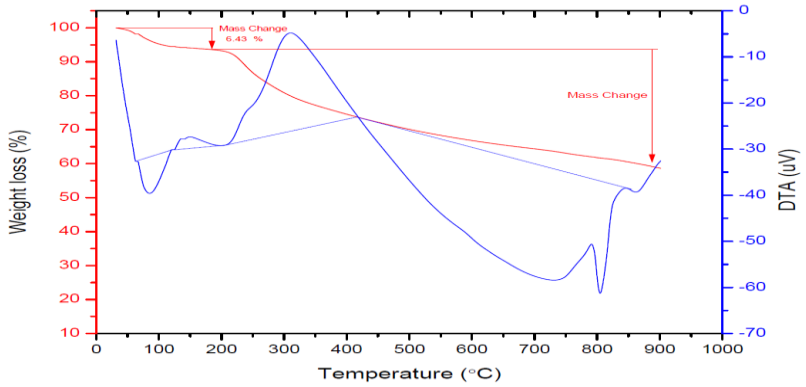


Figure 5. TG graph of CTV ligand.

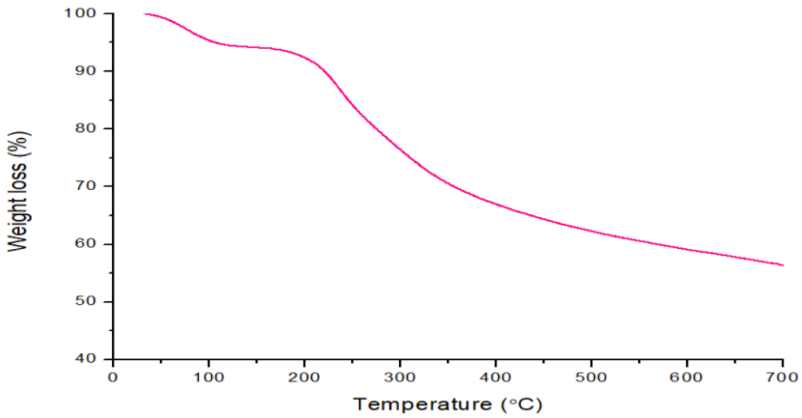


Figure 6. TG graph of CTV-Cu complex.

Compound	Temp. (°C)	Weight Loss (%)	Thermal Event
CTV	**185**	6.43	Loss of water
	200-900	34.57	Chain disruption and backbone degradation

CTV-Cu	**200**	7.56	Loss of water
	200-500	30.10	Disruption of the chain
	500-700	5.75	Further degradation of the backbone

Table 1. TG data of CTV ligand and CTV-Cu complex.

ESR Spectroscopy

The ESR spectrum of the CTV-Cu complex was recorded at room temperature using an X-band spectrometer operating at a microwave frequency range of 8.75–9.65 GHz as shown in Figure 7. revealed no hyperfine splitting, which was ascribed to exchange broadening caused by the inadequate separation of the paramagnetic center at a low X-band frequency of 9.44 GHz. The resultant g value of 2.0440 indicates that the ligand has a moderate field strength with covalent character and exhibits a square planar geometry with N/O donor atoms. Intermolecular spin-spin interactions and dimeric association of molecules contributed to non-resolution of hyperfine features due to copper (S = 1/2 and I = 3/2). However, the spectra that corresponded to an unpaired electron in the $dx^2 - y^2$ orbital of the Cu(II) centers demonstrated a square planar orientation of the complexes, while the spectra in which the g parallel tensors were undetectable with the absence of hyperfine splitting still had the feature to be characterized by axial g tensors. The covalent behavior of the complex, which depended on the density of unpaired electrons in ligand molecules, introduced spin-orbital coupling with unpaired electrons, which caused the g values to change from ge (2.0023).

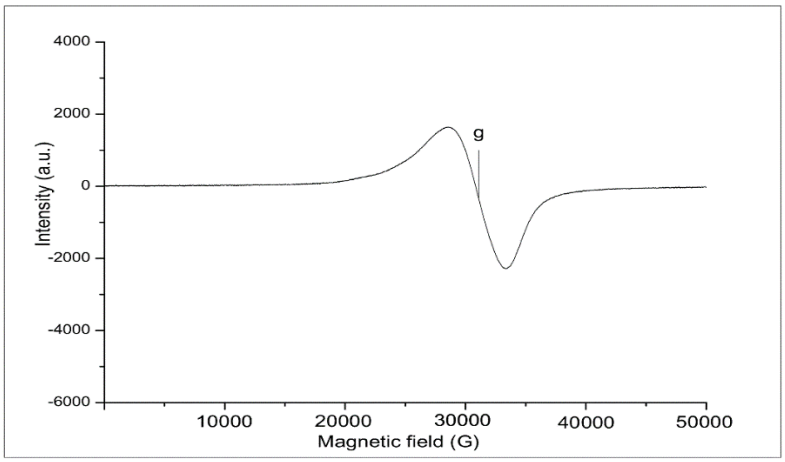


Figure 7. ESR spectrum of CTV-Cu complex.

Magnetic Susceptibility Measurement (Vibrating Sample Magnetometer-VSM)

The VSM of CTV-Cu showed that the magnetization of the material was superparamagnetic, and the values of intrinsic coercivity (H_{ci}), retentivity (M_r), and saturation magnetization (M_s) were 91.246 Oe, 94.464 × 10^{-6} emu, and 1.3763 x 10^{-3} emu, respectively. The molar magnetic susceptibility was found to be 4.87 × 10^{-4} emu mol^{-1} Oe^{-1}. The values, marginally higher than the spin-only value of 1.73 BM, indicate notable spin-orbit coupling in the cupric ions. However, values less than 1.90 BM indicate that the complexes have distorted square planar geometry. The magnetic moment values in the vicinity of the spin-only moment of 1.73 BM corresponding to an unpaired electron provided evidence of the low spin-spin interaction between the unpaired electrons of the copper atoms.

Elemental Analysis (CHNS)

The CHNS elemental analysis of the synthesized CTV ligand revealed the presence of carbon (18.24%), nitrogen (4.17%), sulfur (1.83%), and hydrogen (4.20%). The relatively high carbon content confirms the presence of an

organic backbone derived from chitosan and the vanillin moiety, indicating the successful formation of the Schiff base framework. The observed nitrogen percentage supports the incorporation of thiosemicarbazone functionality, with nitrogen atoms originating from both chitosan amino groups and the thiosemicarbazide unit, which participate in coordination with the metal ions. The presence of sulfur further confirmed the formation of the thiosemicarbazone group (–C=S). Additionally, the hydrogen content is consistent with the presence of hydroxyl, amine, and aromatic protons in the ligand structure.

The CHNS elemental analysis of the synthesized CTV–Cu complex, suggests the presence of carbon (28.67%), nitrogen (6.09%), sulfur (2.00%), and hydrogen (6.42%). The increased carbon content compared to the free ligand confirms the preservation of the organic backbone and suggests successful coordination without degradation of the chitosan–vanillin framework. The nitrogen percentage indicates the involvement of azomethine (–C=N–) and thiosemicarbazone nitrogen atoms, which are coordinated to the copper ion, thereby supporting complex formation. The presence of sulfur further confirmed the retention of the thiosemicarbazone moiety (–C=S), which acts as an important donor site for metal binding and participates in metal binding through sulfur coordination. The observed hydrogen content is consistent with the presence of hydroxyl, amine, and aromatic protons within the structure. Therefore, the CHNS data are in good agreement with the proposed structure of the copper complex, confirming the successful formation of the chitosan-based vanillin thiosemicarbazone copper complex and the coordination of the ligand with the Cu(II) metal center.

NMR Spectroscopy

The ^{13}C NMR spectra (Figure 8) of the chitosan-functionalized Schiff base (CTV) showed a C_2 signal at δ 55.984 ppm, indicating the partial involvement of the amino group. The resonance at δ 174.637 ppm indicates partial deacetylation of the acetamido moiety in chitosan. Additional peaks corresponding to the chitosan backbone were observed at δ 23.245 ppm ($–CH_3$) and δ 61.197 ppm (C_6), while signals for C_3 and C_5 appeared in the range of δ 74.777–76.623 ppm and δ 98.544 ppm to C_1. The overlapping signals observed in the range of δ 174.637–181.362 ppm is attributed to the superimposition of C=S and C=O functional groups. These results conclude that the formation of chitosan thiosemicarbazone with partial fulfilment of the thiosemicarbazone group in chitosan.

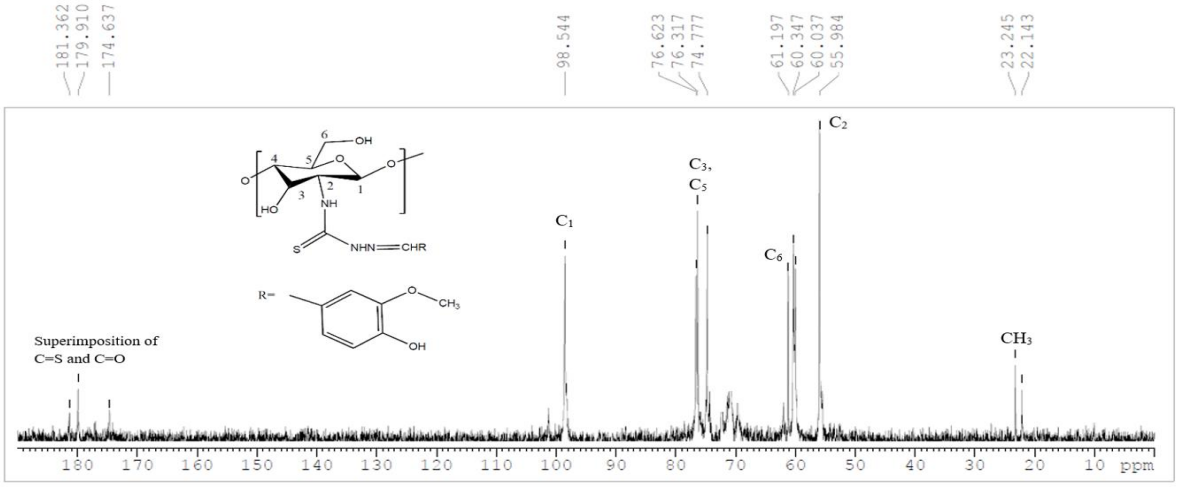


Figure 8. ^{13}C NMR of CTV ligand.

Anticancer Activity

MTT Assay against the MCF-7 Cancer Cell Line

The Michigan Cancer Foundation-7 (MCF7) cell line was cultured in DMEM medium supplemented with 10% inactivated Fetal Bovine Serum (FBS), penicillin (100 IU mL^{-1}), and streptomycin (100 µg mL^{-1}) in a humidified atmosphere of 5% CO_2 at 37°C until confluent. The monolayer cell culture was trypsinized, and the cell density was adjusted to 1 × 105 cells mL^{-1} in medium containing 10% FBS. A 100 µL aliquot of the cell suspension (1 ×

104 cells well^{-1}) was seeded into 96-well plates and incubated for 24 h to allow the formation of a partial monolayer. After removing the supernatant and washing with fresh medium, 100 µL of various concentrations of the test compound was added, followed by incubation at 37°C in a 5% CO_2 atmosphere for 24 h. Subsequently, the medium was replaced with 100 µL of MTT solution (2 mg mL^{-1} in PBS) and incubated for 4 h under the same conditions. The resulting formazan crystals were dissolved in 100 µL of DMSO, and absorbance was measured at 570 nm using a microplate reader. The percentage of cell growth inhibition was calculated, and the IC_{50} values were determined from the dose–response curves for each cell line. The data on the anticancer activity of the CTV-Cu complex was presented in Figure. 9-10 and Table 2, an increase in the sample concentration correlated with a higher rate of cancer cell death.

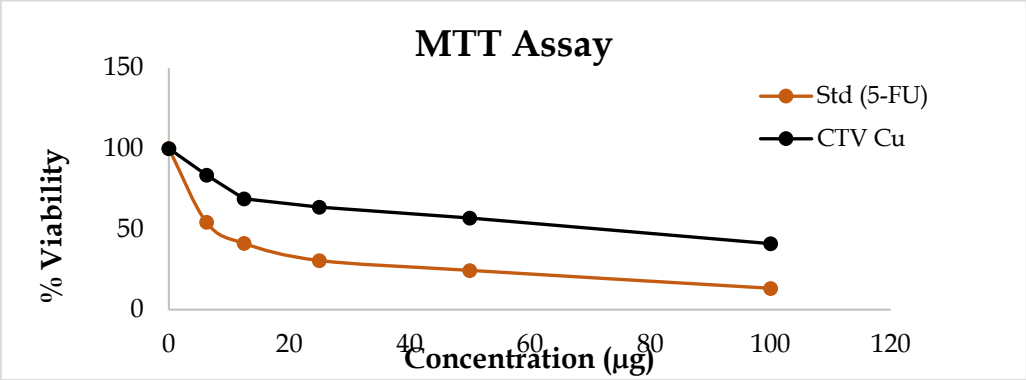


Figure 9. MTT Assay of CTV-Cu complex.

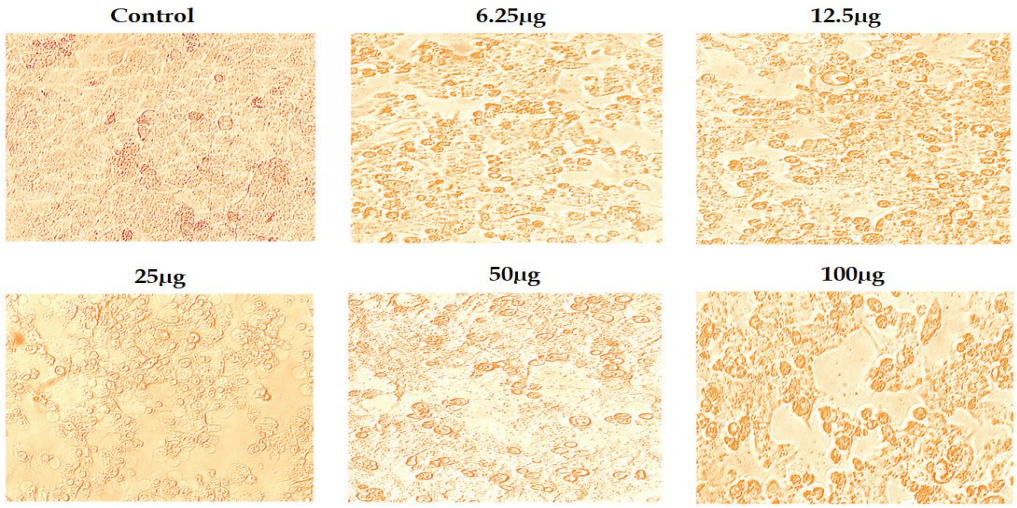


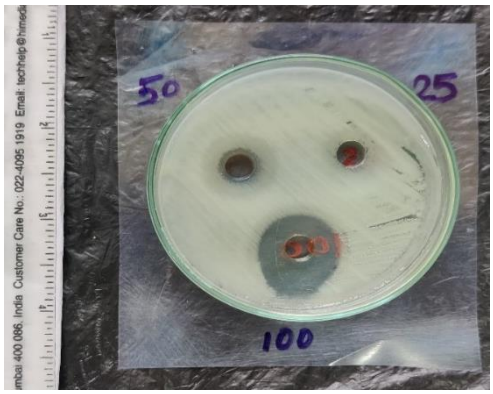
Figure 10. Anticancer activity of CTV-Cu complex (MCF7 cell line).

Conc. (µg/ml)	% viability		SD	
	Std (5-FU)	CTV Cu	Std (5-FU)	CTV Cu
0	100	100	0	0
6.25	54.251	83.535	0.764	0.2
12.5	41.102	68.875	0.841	0.263
25	30.526	63.587	0.997	1.128
50	24.373	56.793	1.076	0.451
100	13.262	40.949	1.039	1.757
IC_{50} (µg)	7.46	62.54		

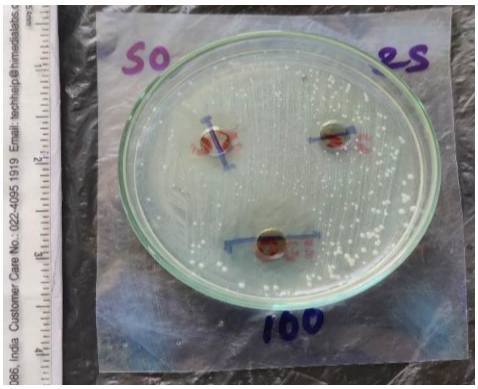
Table 2. Anticancer activity of CTV-Cu complex.

Antibacterial Activity

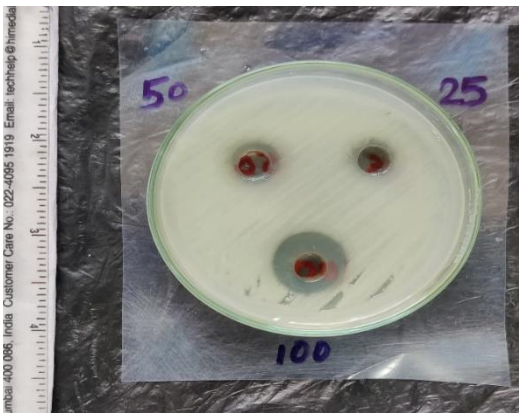
Antibacterial activities of CTV and CTV-Cu (Figure. 11) was performed using the Kirby-Bauer well diffusion method [26]. For this purpose, EC12 *Escherichia coli* (Gram-negative) and SA16 *Staphylococcus aureus* (Gram-positive) bacteria were used for antibacterial studies. The inhibition zones of CTV and CTV-Cu in EC12 and SA16 were observed at different concentrations. The CTV in Figure 12 showed no inhibition at low concentration (25 µL) and found 11 mm (50 µL) and 20 mm (100 µL) inhibition zones against *E. coli*. The zone of inhibition increased to 11, 15 and 23 mm with increasing concentrations of 25 µL, 50 µL, and 100 µL respectively, against *S. aureus*. Figure 13 showed no inhibition against EC12 at a concentration of 25 µL, whereas SA16 exhibited a clear inhibition zone of 14 mm. Increasing the concentration to 50 µL resulted in an 11 mm zone for EC12 and a 17 mm zone for SA16, indicating enhanced activity with dose. At the highest concentration tested (100 µL), the zone of inhibition increased to 17 mm for EC12 and 24 mm for SA16. These results demonstrate that both the CTV and CTV-Cu complexes exhibit concentration-dependent antibacterial activity, with enhanced efficacy observed in the CTV-Cu complex against both Gram-positive and Gram-negative bacteria.



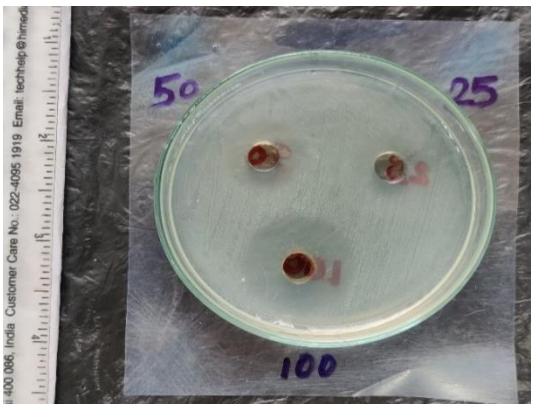
EC12 (CTV)



SA16 (CTV)



EC12 (CTV-Cu)



SA16 (CTV-Cu)

Figure 11. Inhibition zones of CTV and CTV-Cu complex.

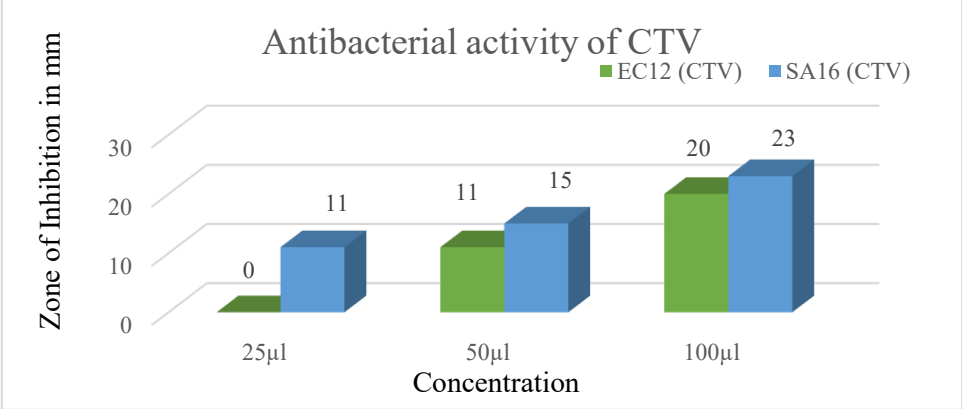


Figure 12. Inhibition zones of CTV ligand at different concentrations.

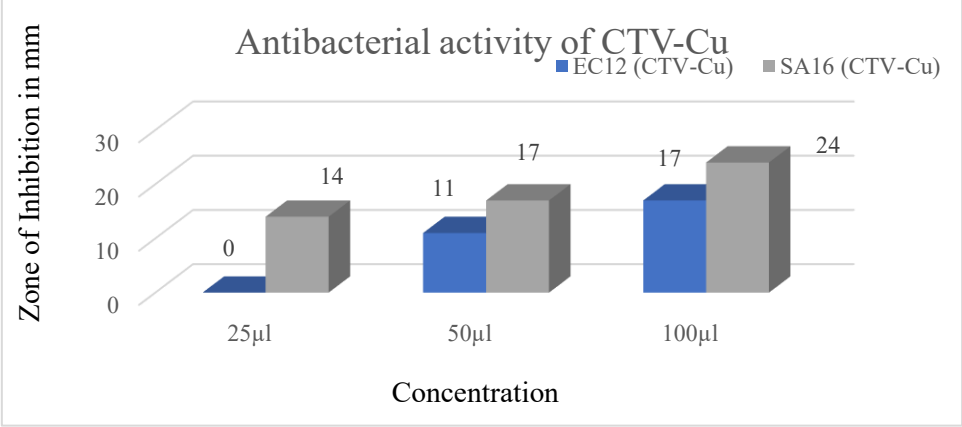


Figure 13. Inhibition zones of CTV-Cu complex at different concentrations.

5. Discussion

The chitosan-functionalized vanillin thiosemicarbazone was prepared using a one-pot synthesis method. The synthesized ligand was then chelated with copper(II) salt, giving a chitosan-functionalized vanillin thiosemicarbazone Cu(II) complex. The synthesized ligand and Cu complex were chemically and structurally characterized using elemental analysis, FTIR, ^{13}C NMR, ESR, magnetic and thermal measurements. This study confirmed that the synthesized ligand and its Cu(II) complex exhibited excellent metal coordination ability, enhanced structural stability, and significantly improved biological and pharmacological activities. Anticancer studies revealed that the copper(II) complex was more effective in MCF-7 cancer cell line proliferation. The antibacterial activities of the complex and ligand were evaluated against Gram-positive and Gram-negative bacteria such as *S. aureus* and *E. coli* using the Kirby-Bauer well diffusion method. These findings suggest that the synthesized chitosan-functionalized vanillin thiosemicarbazone ligand and its Cu(II) complex have great potential for various pharmacological and biological applications.

References

[1] Kedir, W.M., Abdi, G.F., Goro, M.M., and Tolesa, L.D., *Heliyon,* 2022, vol. 8, e10196, p. 1-10. https://doi.org/10.1016/j.heliyon.2022.e10196

[2] Desai, N., Rana, D., Salave, S., Gupta, R., Patel, P., and Karunakaran, B., *Pharmaceutics,* 2023, vol. 15, p. 1-69. https://doi.org/10.3390/pharmaceutics15041313

[3] Kanmani, P., Aravind, J., Kamaraj, M., Sureshbabu, P., and Karthikeyan, S., *Bioresour. Technol.,* 2017, vol. 242, p. 295–303. https://doi.org/10.1016/j.biortech.2017.03.119

[4] Kadouche, S., Farhat, M., Lounici, H., Fiallo, M., Sharrock, P., Mecherri, M., *Waste Biomass Valor.,* 2016, vol. 8, p. 401–6. https://doi.org/10.1007/s12649-016-9593-2

[5] Hisham, F., Akmal Maziati, M.H., Ahmad, F., Ahmad, K., and Samat, N., *Ain Shams Eng. J.,* 2024, vol. 15, p. 102-424. https://doi.org/10.1016/j.asej.2023.102424
[6] Huq, T., Khan, A., Brown, D., Dhayagude, N., He, Z., and Ni, Y., *J. Bioresour. and Bioprod.,* 2022, vol. 7, p. 85–98. https://doi.org/10.1016/j.jobab.2022.01.002
[7] Badawy Mohamed, E. I., and Rabea, Entsar, I., *Int. J. Carbohydr. Chem.*, 2011, vol. 2011, p. 1-29. https://doi.org/10.1155/2011/460381
[8] Vadivel, T., Dhamodaran, M., Kulathooran, S., Kavitha, S., Amirthaganesan, K., Chandrasekaran, S., Ilayaraja, S., and Senguttuvan, S., *Carbohydr. Res.,* 2020, vol. 487, p. 107-878. https://doi.org/10.1016/j.carres.2019.107878
[9] Suresh, R., Moganavally, P., Deepa, M., and Sudha, P.N., *Orient. J. Chem.,* 2016, vol. 32, p. 2509–16. https://doi.org/10.13005/ojc/320521
[10] Singh, N., and Yadav, S.S., *Inorg. Chem. Commun.,* 2024, vol. 167, p. 112-724. https://doi.org/10.1016/j.inoche.2024.112724
[11] El-Khawaga, A.M., Farrag, A.A., Elsayed, M.A., El-Sayyad, G.S., and El-Batal, A.I., *J. Clust. Sci.,* 2020, vol. 32, p. 1107–19. https://doi.org/10.1007/s10876-020-01869-6
[12] El-Sayed, D.S., Hassan, S.S., Jassim, L.S., Issa, A.A., Al-Oqaili, F., Al-Bayaty, M.K., Hasson, B.A., Jabir, M., Habeeb, K., and Elbadawy, H.A., *BMC Chem.,* 2025, vol. 19, p. 1-26. https://doi.org/10.1186/s13065-024-01338-5
[13] Celik, E., Ozdemir, M., Köksoy, B., Taskin-Tok, T., Taslimi, P., Sadeghian, N., and Yalcin, B., *ChemistrySelect,* 2023, vol. 8, p. 1-13. https://doi.org/10.1002/slct.202301786
[14] Mohamed, N.A., Mohamed, R.R., and Seoudi, R.S., *Int. J. Biol. Macromol.* 2014, vol. 63, p. 163–69. https://doi.org/10.1016/j.ijbiomac.2013.10.044
[15] Miller, M.C., Stineman, C.N., Vance, J.R., West, D.X., and Hall, I.H., *Anticancer Res.,* 1998, vol. 18, p. 4131-9. https://pubmed.ncbi.nlm.nih.gov/9891458/
[16] Agrawal, K.C., and Sartorelli, A.C., *In Prog. Med. Chem.,* 1978, vol. 15, p. 321-356. https://doi.org/10.1016/s0079-6468(08)70259-5
[17] Adhikari, H.S., Garai, A., Khanal, C., Adhikari, R., and Yadav, P.N., *Asian J. Chem.,* 2021, vol. 33, p. 969–76. https://doi.org/10.14233/ajchem.2021.23078
[18] Adhikari, H.S., Gavai, A., Thapa, M., Adhikari, R., and Yadav, P.N., *J. Macromol. Sci., Part A.,* 2022, vol. 59, p. 211–27. https://doi.org/10.1080/10601325.2021.2022982
[19] Adhikari, H.S., Garai, A., Manandhar, K.D., and Yadav, P.N., *ACS Omega,* 2022, vol. **7** p. 30978–88. https://doi.org/10.1021/acsomega.2c02966
[20] Adhikari, H.S., Garai, A., and Yadav, P.N., *Carbohydr. Res.,* 2023, vol. 526, p. 108-796. https://doi.org/10.1016/j.carres.2023.108796
[21] Adhikari, H.S., *J. Eng. Sci.,* 2024, vol. 3, p. 1–8. https://doi.org/10.3126/jes2.v3i1.66226
[22] Adhikari, H.S., Garai, A., Khanal, C., and Yadav, P.N., *Carbohydr. Polym. Technol. Appl.,* 2024, vol. 7, p. 100-469. https://doi.org/10.1016/j.carpta.2024.100469
[23] Haj, N.Q., Mohammad, M.O., and Alkubaisi, H.M.M., *Results Chem.,* 2024, vol. 12, p. 101-859. https://doi.org/10.1016/j.rechem.2024.101859
[24] Vadivel, T., and Dhamodaran, M., *Int. J. Biol. Macromol.,* 2015, vol. 90, p. 44-52. https://doi.org/10.1016/j.ijbiomac.2015.11.008
[25] Vadivel, T., Dhamodaran, M., Kulaathooran, S., Kavitha, M., and Amirthaganesan, K., *Curr. Appl. Polym. Sci.,* 2019, vol. 3, p. 212-220. https://doi.org/10.2174/2452271603666191016130012
[26] Bauer, A.W., Kirby, W.M., Sherris, J.C., and Turck, M., *Am. J. Clin. Pathol.* 1966, vol. 45, 493-96. https://doi.org/10.1093/ajcp/45.4_ts.493